# INTEREST OF 3D MODELING FOR LAI RETRIEVAL FROM CANOPY TRANSMITTANCE MEASUREMENTS: THE CASES OF WHEAT AND VINEYARD

**B. de Solan**

*ARVALIS - Institut du végétal*
*3, rue Joseph et Marie Hackin, 75116 PARIS, France*

**R. Lopez-Lozano, K. Ma, F. Baret**

*INRA - EMMAH UMR 1114*
*Domaine Saint Paul, Site Agroparc, 84914 Avignon, France*

**B. Tisseyre**

*Montpellier SupAgro - UMR ITAP*
*2 place Pierre Viala, 34060 Montpellier Cedex 02, France*

## ABSTRACT

LAI is one of the most appealing crop measurement required by agronomists to develop methods for decision making in agriculture. This study presents ways to estimate LAI from indirect measurements, with emphasis on the interest of using a 3D representation of canopy architecture as compared to more simple 1D models. The work is restricted to gap fraction measurements which are now easy to achieve at the ground level. Wheat and vineyard contrasted canopies are considered. The 3D models for wheat and vineyard are first presented and used to simulate a wide range of canopy architecture under several geometrical measurement configurations. Results showed that the assumption of random distribution of leaves in 1D models are only applicable for a limited sets of observational configurations such as perpendicular to rows and with medium to large zenith angles. 3D models have a much larger domain of validity. Further, introducing some priori information on canopy architecture (such as the row characteristics) improves the performances and counterbalanced the increase number of variables required by the 3D models. These results primarily derive from model simulations were then validated using measurements over actual wheat and vineyard crops. They confirm the theoretical findings.

**Keywords:** Leaf Area Index (LAI), 3D models, canopy transmittance

## INTRODUCTION

Remote sensing is a powerful tool for crop monitoring. Its main interest relies on its ability to provide non destructive estimates of some key biophysical variables. Several observation systems offer spatial and temporal resolution compatible with agronomic management requirements. Spatial resolution depends mainly on vectors hosting the sensors. A wide range of

vectors is used for agricultural applications: handheld systems, tractors, airplanes unmanned or not, and satellites.

Among the biophysical variables accessible from remote sensing measurements, leaf area index (LAI) is of particular interest since it controls crop growth through light interception, and transpiration while resulting from crop development integrated until the measurement date.

A wide range of sensors and associated methods exist to estimate LAI from indirect measurements. They are generally based on canopy reflectance (Baret et al., 2007; Moran et al., 1997) or transmittance (Chen and Cihlar, 1995; Jonckheere et al., 2004). A first class of estimation strategies use empirical relationships especially based on spectral indices. Their main limitation is their lack of generality and the need for ground calibration to account for the multiple other factors influencing reflectance. A second approach is based on simple radiative transfer models that simulate canopy transmittance or reflectance for a given set of characteristics of the canopies including LAI. Model inversion techniques allow then retrieval of these biophysical variables from a set of radiometric measurements. However, the simplifications and assumptions on canopy structure representation associated to these models may lead to inaccurate LAI estimates.

A powerful way to overcome these limitations is to use three dimensional (3D) models. They offer an explicit description of the canopy structure. If the first versions were essentially static (Espana et al., 1999), some of them recently developed are dynamic. They take into account environmental drivers including light and temperature. Computer and hardware efficiency allow fast generation of the virtual 3D scenes. At the same time, radiative transfer models based on ray tracing or radiosity methods (Disney et al., 2003) have been developed to simulate photons' path in the canopy, for a given 3D scene and a given solar configuration. They thus provide very accurate canopy reflectance and transmittance simulations.

This work will focus on gap fraction measurements in the canopy to estimate LAI. Gap fraction corresponds to light transmittance in the particular case of black leaves. Several devices based on digital photography or light sensors working in the blue spectral domain have been developed to measure gap fraction. However, the transformation of these measurements into LAI heavily depends on canopy architecture. The objectives of this work are to show the interest of 3D dynamic models as compared with 1D simple models to retrieve LAI in the case of two very different crops: wheat and vineyard. The way virtual scenes are generated is first detailed as well as the techniques used to compute gap fraction. Then, simulations of gap fraction with a 1D model for different viewing configurations are compared with simulations with an explicit 3D model. Sensitivity analyses to canopy variables as well as measurement configuration are presented for both crops. They allow designing optimal configurations and methods to estimate LAI from gap fraction. Finally, results from these theoretical considerations are validated using dedicated field experiments.

## METHODS AND TOOLS TO SIMULATE AND INTERPRET INDIRECT MEASUREMENTS

### The 1D model: a simplification of the canopy

Most of the devices designed for LAI indirect estimation rely on light transmittance measurement through the canopy. LAI is related to the gap fraction, Po(θ), for a given view zenith angle θ using the Beer's law That relies on 1D structure description considering the canopy as a turbid medium with randomly distributed small leaves:

$$\mathrm{Po}(\theta) = \exp(-\mathrm{k}.\mathrm{PAI}) \quad [1]$$

Where k is the extinction coefficient that is calculated as:

$$k = \frac{G(\theta s, LIDF)}{cos(\theta s)} \quad [2]$$

where G(θs,LIDF) is the projection function, i.e. the mean projection in the direction θs of a unit leaf area. LIDF is the Leaf Inclinations Distribution Function that may conveniently be approximated by an ellipsoidal leaf angle distribution, or calculated from digitised plants.

## The wheat 3D model

Adel-wheat (Fournier et al., 2005) is a dynamic architectural model of wheat, based on the L-system principles (Prusinkiewicz, 1999). In Adel-wheat, the phytomer is the basic unit. It consists in a leaf, inserted on a node, an internode and a tiller bud. Each phytomer is described by a set of triangles. At the stand level, planting pattern is described by a seedling density and an inter row distance. From this set of variables, the model describes the size, shape, and orientation in space of each organ of a plant population as a function of degree days above 0°C. The Adel Wheat model is a package included in the OpenAlea platform (Pradal et al., 2008).

The Adel-Wheat model was calibrated over several experiments (Evers et al., 2007). Some of the parameters (leaf blade curvature and orientation in space) are stochastic, based on experimental distribution laws.

From this database, a total of 432 scenes were simulated by varying some of the main variables driving wheat canopy architecture. The other variables were set to realistic values. Scenes are made of 6 rows of one meter.

**Table 1. Structure parameters for ADEL-wheat model manipulated in the simulated scenes.**

| Parameters (units) | Value levels |
|---|---|
| Thermal time (°C.d) | 400, 600, 800, 900, 1000, 1200 |
| Plant density (plant/m$^2$) | 150, 300, 500 |
| Number of tiller per plant | 2, 4 |
| Distance between the top of tiller and main stem (cm) | 3, 6 |
| Height of plant | low, medium, high |
| Leaf inclination distribution (drawn from actual measurements) | plagiophile, erectophile |

## The vineyard 3D model

A geometrical approximation has been considered to represent actual vertically-trained vineyards. The proposed model describes the vineyard rows as parallelepiped prisms, assuming that leaf distribution inside the row is homogeneous. These rows are defined by width W and height H, and are separated from a distance $D_{rows}$. Trunks are represented by eight triangles with a height $H_{trunk}$ and a distance $D_{plants}$ along the row (Fig. 1).

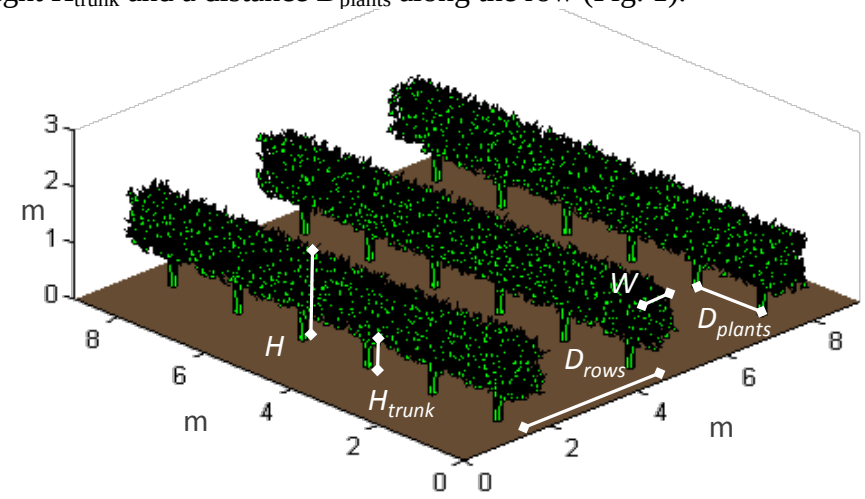


**Fig. 1. An example of a vineyard 3D scene.**

The leaves are represented by isosceles triangles with a base of 10 cm and a height of 15 cm. The LIDF follows an erectophile distribution and the number of leaves within the rows is determined by canopy LAI.

Although more detailed models of vineyard architecture can be found in literature (Louarn et al., 2005), representing the leaves grouped in branches and following a given trajectory, the geometrical approach proposed constitutes a good compromise between realism and the ease of use, since it requires a limited number of input variables.

The proposed model was used to create a total of 3420 scenes combining orthogonally the possible variations in the field of the above mentioned input parameters. This experimental plan comprises an extreme range of canopy characteristics: from 1D description when $W=D_{rows}=1.5$ to highly clumped canopies ($D_{rows}=4$; $W=0.3$).

## Computation of gap fractions from 3D scenes

LAI is defined as half the total developed area of green leaves per unit horizontal ground area (Chen and Black, 1992). Calculated LAI is the sum of the leaves' one sided triangles areas. Note that for most of the sensors, only PAI (Plant Area Index) is accessible as no discrimination can be done between leaves and the other canopy elements. PAI includes half the developed area of the branches, stems and reproductive organs. The green area index (GAI) considers only the area of green elements. For the simulations considered here, PAI = GAI since senescence is not represented.

Gap fraction ($P_0$) calculation is computed using the Z-buffer technique (Chelle, 1997). It consists on an orthogonal projection of the scene onto a grid.

Each pixel value is the depth of the triangle on the grid. $P_0$ is calculated for the scene as the ratio between maximum depth (soil pixels) and the total amount of pixels of the grid. To avoid border effects, scenes are replicated infinitely (Chelle et al., 1998).

In the case of vineyard canopies, $P_0$ was calculated from 0° to 85° in zenith directions and from 0° to 90° in azimuth directions (0° equals to rows direction) using the Z-buffer technique. $P_0$ values were integrated in sectors trying to mimic the optical configurations available in LAI2000 instrument. LAI2000 is equipped with 5 concentric sensors with an IFOV of 15° in zenith, centred at 7.5°, 22.5°, 37.5°, 52.5° and 67.5° and 360° in azimuth. However, azimuth viewing can be constrained using two caps that limit the IFOV to 90° and 45° around to a specific direction. Fifteen optical configurations were thus reproduced from $P_0$ simulations: the five concentric rings of LAI2000 by 3 azimuth amplitudes: IFOV of 360°, and 90° and 45° centred to direction perpendicular to rows.

## DIFFERENCE BETWEEN 1D AND 3D FOR GAP FRACTIONS

To show the importance of canopy architecture effects on the interpretation of indirect measurements, comparisons between the 1D simulations and a realistic 3D model are presented below for wheat and vineyard.

### The case of a wheat canopies

From each 3D scene, PAI and LIDF were calculated. Both information were used to simulate Po with the 1D model for two viewing configurations: (i) a viewing azimuth angle of 57.5° parallel to the rows direction; (ii) a viewing azimuth angle of 57.5° perpendicular to the rows direction.

Comparison between both models simulations (Fig. 2) shows that the 1D model fails to represent accurately some viewing configuration. In particular, when the viewing azimuth angle is parallel to the row, the turbid medium assumption is not fulfilled. On the other hand, a good agreement is observed between the 1D and 3D models when the azimuth is perpendicular to the rows. This is the optimal condition to use the 1D model.

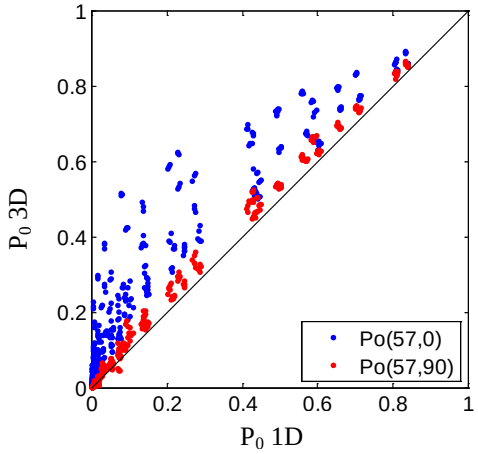


**Fig. 2. Comparison between simulated gap fractions from the 1D model and the 3D Adel Wheat model for 2 viewing configurations with a**

**viewing zenith angle of 57.5°: in blue azimuth is parallel to the rows direction and in red it is perpendicular to the rows**

## The case of vineyard

The discontinuity of vineyard canopies invalidates the application of 1D assumption to establish the relationship between LAI and intercepted light. As it can be appreciated in Fig. 3a, the actual gap fraction of vineyard canopies ($P_0$ 3D) presents large differences with that of the 1D canopy with the same LAI ($P_0$ 1D).. The effect of the canopy discontinuity limits the sensitivity of $P_0$3D to LAI (Fig. 3c), and enhances the contribution of other architectural variables such as rows width and height. In other words, light transmission is not determined only by the amount of leaf area, but also on the way leaves are distributed in the canopy.

Measurement direction is another factor that drives transmittance values. For directions close to zenith and/or parallel to rows direction (Figure 3a and 3c), the effect of canopy architecture is the largest. For directions perpendicular to the rows and far from zenith, the 1D description approach may be valid (Fig. 3b).

The contribution of canopy architecture variables other than LAI or LIDF such as row dimensions and height should be explicitly considered and if possible introduced in the inversion process.

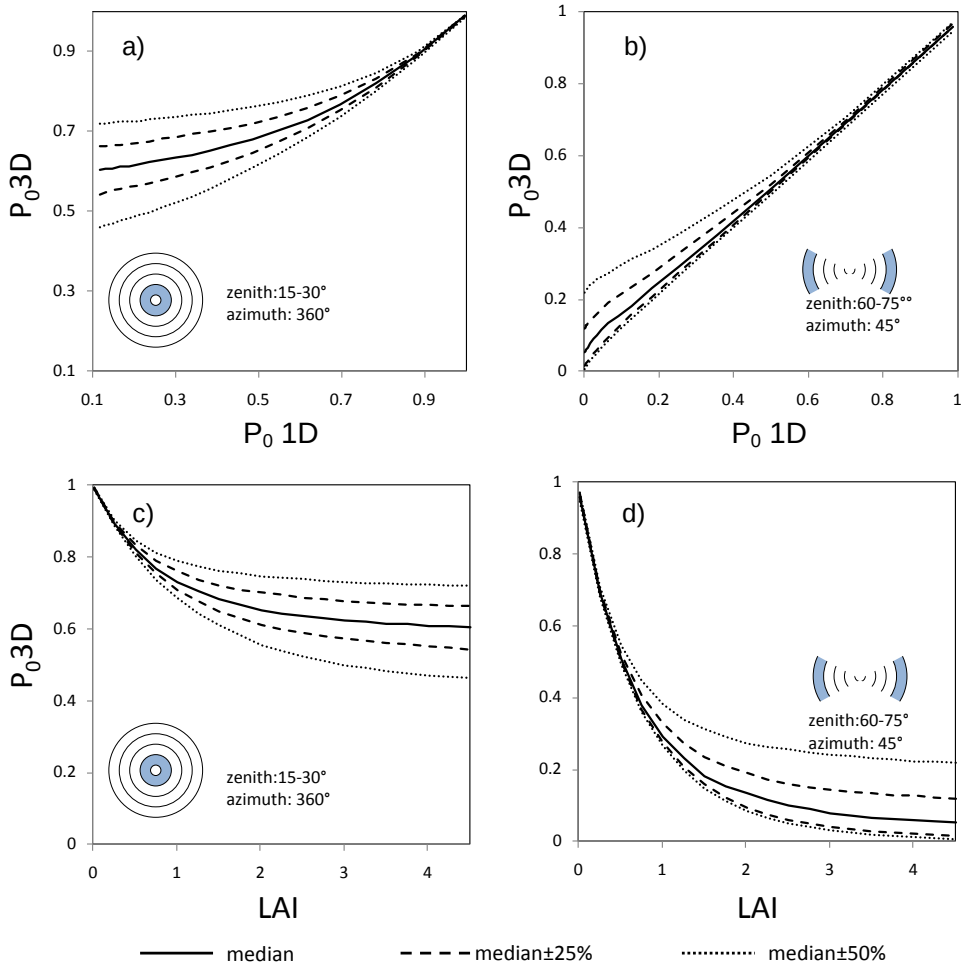

**Figure 3. Top figures (a, b): distribution of $P_0$ values simulated with the 3D vineyard model against $P_0$ of an equivalent canopy in 1D model. Bottom figures (c, d): relationship between $P_0$ simulated by the 3D model and LAI. Two geometrical configurations of the LAI2000 instrument were considered: on the left all azimuth are considered, but zenith is restricted to the 15°-30° range. On the right azimuth are restricted to directions ±22.5° perpendicular to the rows.**

## VIEWING CONFIGURATION OPTIMIZATION AND ASSOCIATED ESTIMATION METHODS: FROM SIMULATIONS TO THE FIELD

### LAI estimate from single direction gap fraction measurement on wheat

#### Calibration of a relationship between PAI and gap fraction at 57.5°

Wilson (1963) demonstrated that the projection function can be considered as independent of leaf inclination at $\theta_s$=57.5°. $G(\theta_s)$ is almost constant and equals 0.5.

In this configuration, PAI can be retrieved from $Po(57.5°)$ using a simple equation (Weiss et al., 2004):

$$Po(57.5°) = e^{-\frac{0.5 \cdot PAI}{\cos 57.5°}} \Leftrightarrow PAI = -\frac{\cos 57.5°}{0.5} \log(Po(57.5°)) \qquad [3]$$

The gap fraction computed over the 432 simulated wheat canopies were related to the corresponding PAI values. Fig4 a shows that the particular configuration considered at 57.5° zenith angle and perpendicular to the rows minimizes all the sources of variability of canopy architecture introduced in the simulated scenes according to table 1. Very little scatter is observed around the best fit curve adjusted with the simplex optimization method ($R^2$=0.97; RMSE=0.014):

$$Po(57) = e^{-0.824 \cdot PAI} \quad [4]$$

In this case, the use of 3D models allows defining an appropriate viewing configuration and a unique relationship between an indirect measurement, the gap fraction at 57.5°, and a biophysical variable, the PAI. It should however be noted that this relation presents a saturation effect for PAI greater than 3 to 4: application of this equation for more developed crops may lead to inaccurate results.

#### Field experiment

Three experiments were conducted in Boigneville, France (47.33° N; 2.38° E) from 2006 to 2008 resulting in a total of 28 measurements. Seven wheat cultivars (*Triticum aestivum*) and one triticale cultivar (*Triticosecale)* were sampled over plots at several stages from sowing to earing. The investigated plots were very homogeneous microplots of about 2 m width by 10 m long. Destructive LAI was measured by collecting all the plants over 50x50 cm² samples for the earlier stages and on 100x34 cm² for the latter

ones. The area of stems and ears per unit soil area was also measured to compute the PAI.

Pictures were taken with a Nikon D40 hosting a 23.7 x 15.6 mm CCD matrix of 6.24 million pixels, and equipped with a 35mm focal length lens. The 57.5° zenith angle was obtained using a platform inclined at 57.5° bearing a bubble level. Pictures sampled the centre of the plot perpendicularly to the rows so that approximately the same canopy volume was sampled by the photo and by the destructive method. A binary classification of green elements and gaps (including soil and senescent elements) was then performed to compute the gap fraction at 57.5°. The Can-eye freeware was used to achieve the classification) based on the colour space.

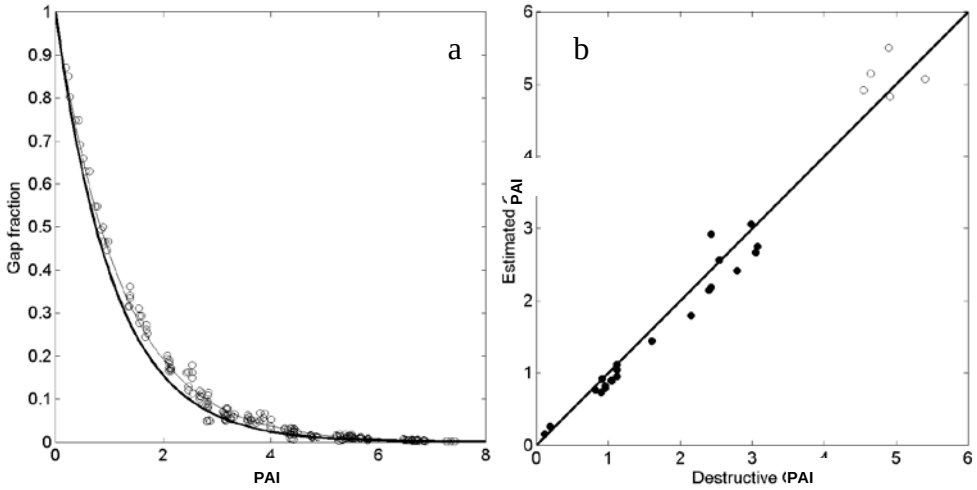


**Fig. 4. a) Relationship between gap fraction at 57.5° and PAI simulated from ADEL-wheat. The thin solid line corresponds to the best exponential fit (equation [4]). The thick solid line corresponds to the theoretical relationship of equation [3]: $\mathbf{Po(57.5^{o}) = e^{-0.931 \cdot GAI}}$.**
**b) Comparison between destructive $GAI$ measurements and estimates of $GAI$ from $P_0$(57.5°) measurements and equation [4]. Filled circles correspond to stages before stem elongation while empty circles represent measurements at flowering stage.**

## Results

GAI estimated from gap fraction measured at 57.5° using equation [2] calibrated with the 3D ADEL-wheat model simulations is strongly correlated to destructive PAI from the 28 field measurements (Fig. 4b), with a RMSE of 0.22. Using equation 1 from 1D model degrades the RMSE to 0.39. The independency of the method from architecture effects is thus well demonstrated over a range of cultivars with contrasted leaf inclinations, at different stages and level of PAI.

## LAI estimation in vineyard canopies from hemispherical photography

### Optimal viewing configuration and neural network training

A unique relationship cannot apply for all architectures simulated for vineyard. In this case, the dataset of gap fraction simulations on 3D vineyard canopies previously described were used to train artificial neural networks (ANN) to estimate LAI from observed $P_0$3D values following different configurations of the LAI2000 instrument. A total amount of 60 ANNs, as it results of combining the simulated $P_0$3D observations with 1 to 4 adjacent rings at the same time multiplied by 1 to 3 adjacent azimuth fields of view: 360°, 90° and 45° perpendicular to rows and 2 types of training datasets: with and without architectural information. In the training dataset without architectural information (from now 'non architectural', only simulated $P_0$3D data was used for the training of ANNs, with LAI as the target. Thus the length of the input vector in the training process would vary from 1 (1 ring) up to 4 (4 rings used at the same time with 1 cap).

In the training dataset with architectural information (from now 'architectural') $P_0$3D simulated data were introduced as well as the respective relative row dimensions $H/D_{rows}$ and $W/D_{rows}$ in the virtual scenes and LAI as target variable. The values of $P_0$3D and row dimensions used for ANN training were contaminated with a random white noise assuming error measurements of gap fraction and uncertainties on row dimensions. A classical feed-forward network with one hidden layer made of 5 tangent sigmoid transfer function neurons and one output layer with 1 linear transfer function neuron was selected for this purpose. Levenberg-Marquardt algorithm was used for the training process. The software used in this process was Matlab package (Mathworks Inc, USA).

**Field experiment**

Two experimental field plots of vineyard (cultivars Grenache and Syrah) were selected at Chateauneuf de Gadagne (43.55ºN, 4.16ºE) within the Rhone Valley at south-eastern France. The planting pattern ranges from 2.25-2.5 m. between rows and from 1 to 1.23 meters between plants. A total of four transects were carried out with series of 10 hemispherical photographs covering the inter row spaces at flowering, veraison and vintage phenological stages. The camera used was a Nikon Coolpix 4500 digital camera equipped with a fisheye lens. The series of hemispherical digital images were downloaded and processed with CAN-EYE software to calculate the gap fraction. In the processing of hemispherical photographs, only zenith directions from 0° to 60° were considered, since above 60° from zenith the lack of resolution in the photograph limits the accuracy of the gap fraction retrieval. Values of $P_0$ were integrated in crown sectors mimicking the optical configurations of LAI2000 instruments.

After the acquisition of each series, 21 primary axes -equivalent to 3 complete plants- were selected randomly at each transect. The axes were cut and defoliated and their leaf area was measured using a planimeter. The width and height of the rows at the same locations were also manually determined.

**Results**

Observed values of $P_0$ in the hemispherical photographs were introduced in the ANNs described above. In the case of ANN with 'architectural' training dataset, the row dimensions measured in the field were also introduced to

produce LAI estimations. 'Effective LAI' was also calculated using CANEYE software from hemispherical photographs.

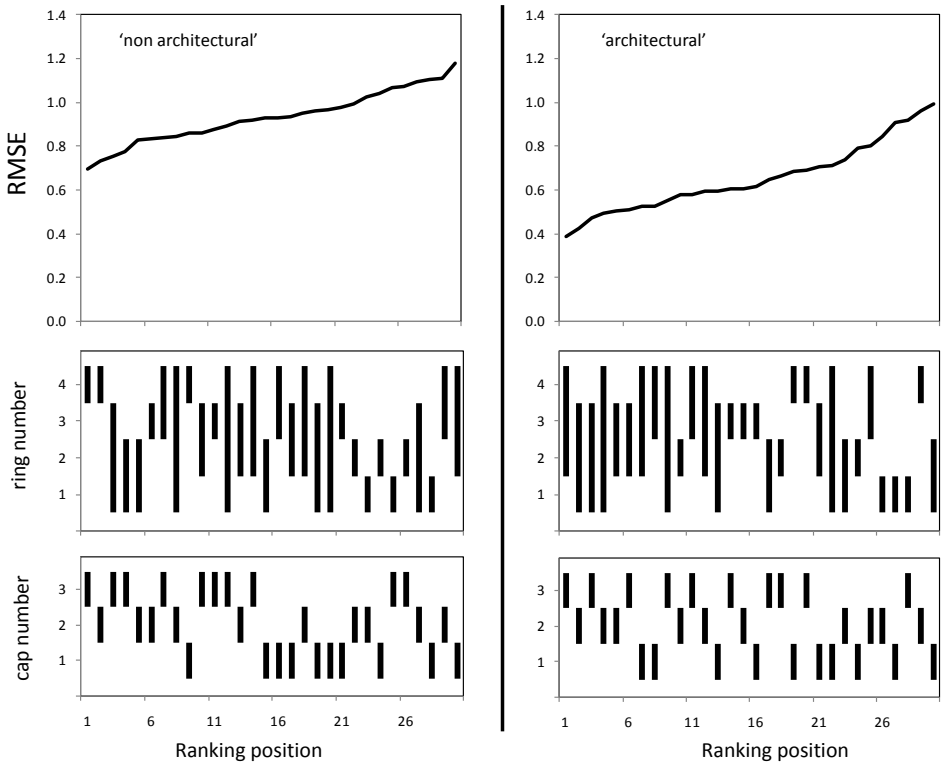


**Fig. 6. RMSE of LAI estimation with ANN using 'architectural' and 'non architectural' training datasets over actual vineyard canopies. The results are ranked from the lowest to the highest RMSE in each case, and the corresponding optical configuration is described in bars.**

When no architectural information is introduced in the training process, the optical configurations that provide better results are those including ring 4 and caps 2 and 3. Although different rings combinations appear among the best performances in LAI estimation, the introduction of azimuth constraints greatly enhances LAI estimation while the configurations including cap number 1 provide systematically poorer performances. Excluding azimuth directions parallel to the rows from the estimation process limits the contribution of architectural parameters while enhancing the sensitivity to LAI.

When canopy architecture information is introduced in the model inversion process, the performances in LAI estimation are greatly enhanced: overall RMSE is substantially improved (Figure 7).

Finally, the performances of ANN estimations were compared against 'effective LAI' estimations assuming 1D model (Fig. 7). Effective LAI is systematically than the observed LAI values, with a RMSE of 0.97. The assumption of a random leaf spatial distribution in 1D model is obviously violated in the case of row crops.

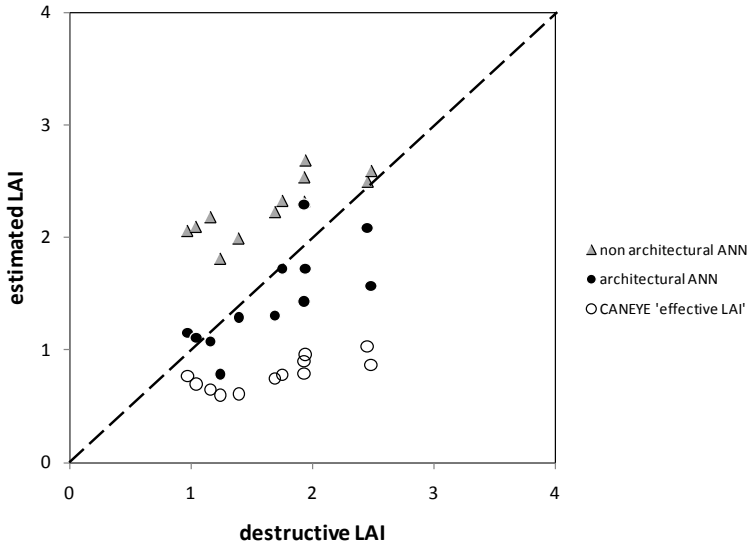


**Fig. 7. Comparison between destructive and estimated LAI by ANNs and CANEYE. Non architectural and architectural ANN refers here only to the best ranked configuration on each category.**

The results of the present experiment suggest the need of using specific optical configurations to estimate LAI on vineyard canopies to mitigate the effect of uncertainties associated to canopy architecture parameters in relation between LAI and intercepted light. Moreover, architecture 3D models in the description of light-canopy interactions has been proved their usefulness in the particular case of vineyard canopies, enhancing the sensitivity of intercepted light to LAI and limiting the influence of other architecture parameters.

## CONCLUSIONS AND PERSPECTIVES

This work presents the simulations of 3D architecture of wheat and vineyard canopies, from a limited set of parameters. The interest of this 3D modelling over the generally used 1D model was demonstrated from simulations and validated over experimental data. Optimal viewing configurations and associated estimation algorithms were derived from a set of simulated canopies showing a large range of architectures.

This analysis for two crops with contrasted architectures allowed defining the conditions of application of the 1D model: it requires that light passes entirely through the canopy, avoiding large gaps between rows and between plants in the rows. This is only achieved for directions far from zenith and perpendicular to rows. This is a key point for younger stages of development in the case of wheat. It is even critical for vineyards. However, a trade off is to be found between the saturation effect enhanced at oblique view angles and the fulfillment of 1D hypotheses that is rarely satisfied with a nadir view angle, except for dense and well developed crops. Combining several view zenith angles is mandatory to alleviate both limitations.

This study also demonstrated the benefit of introducing prior knowledge such as row dimensions on canopy architecture in the model inversion process. Using prior information on canopy architecture allows using more realistic models while compensating for their increased complexity and number of inut variables which is critical in a model inversion process.

Inversion procedures to derive biophysical variables from indirect measurements presented in this paper are not covered exhaustively. Multiple techniques are possible: (i) the easiest is to establish a specific calibration like in the case of wheat presented above and more developed in (Baret et al., In press); (ii) (Casa et al., 2010) minimizes a cost function for parameter estimation; (iii) artificial neural network training is presented in the present article. See also (Lopez-Lozano et al., 2009); (iv) look up tables (LUT) have been successfully applied with reflectance (Knyazikhin et al., 1998) and gap fractions (Garrigues et al., 2008; Weiss et al., 2004). This is a flexible way to account for heterogeneous sources of data.

Although the present study focused on gap fraction, the conclusions can be extrapolated to canopy reflectance, since light transmittance is one of the main components of the radiative transfer models used to compute canopy reflectance. In particular, the effects of sun-target-sensor geometry and row dimensions can largely affect biophysical parameters estimation.

Effective systems for crop monitoring are likely to require multiple types of sensors to increase the amount of information on the canopy. The synergy between radiometers, cameras, lidars or radars can therefore be exploited and an explicit description of canopy structure allows an optimal combination of these data. This approach may solve the well known ill posed problem mentioned by (Combal et al., 2003) when estimating simultaneously LAI and leaf chlorophyll content from reflectances.

Some questions are still open concerning architectural models. (Lewis, 2007) identifies two questions about the use of structural functioning models in remote sensing: (i) what is the impact of the level of detail for the 3D description and (ii) how species dependants are the 3D models? They should be addressed in the next years, with the development of more detailed architectural representations (including for instance leaf twist and undulation) and the integration of other structural crop models in platforms such as OpenAlea.

## ACKNOWLEDGEMENT

B. de Solan gratefully acknowledges the funding of his stay in Avignon from INRA. Many thanks to the developer community of OpenAlea, especially C. Fournier and C. Pradal for their efficient support and to M. Weiss for the developed tools to digitize plant silhouettes.

## REFERENCES

Baret, F., de Solan, B., Lopez-Lozano, R., Ma, K. and Weiss, M., In press. GAI estimates from 57.5° zenith angle downward looking digital photos across rows for row crops. Theoretical considerations based on 3D architecture models and application to wheat crops, Agricultural and Forest Meteorology.

Baret, F., Houles, V. and Guerif, M., 2007. Quantification of plant stress using remote sensing observations and crop models: the case of nitrogen management. Journal of Experimental Botany, 58(4): 869-880.

Casa, R. et al., 2010. Estimation of maize canopy properties from remote sensing by inversion of 1-D and 4-D models. Precision Agriculture.

Chelle, M., 1997. Développement d'un modèle de radiosité mixte pour simuler la distribution du rayonnement dans les couverts végétaux, Université de Rennes, 161 pp pp.

Chelle, M., Andrieu, B. and Bouatouch, K., 1998. Nested radiosity for plant canopies. Visual Computer, 14(3): 109-125.

Chen, J.M. and Black, T.A., 1992. DEFINING LEAF-AREA INDEX FOR NON-FLAT LEAVES. Plant Cell and Environment, 15(4): 421-429.

Chen, J.M. and Cihlar, J., 1995. QUANTIFYING THE EFFECT OF CANOPY ARCHITECTURE ON OPTICAL MEASUREMENTS OF LEAF-AREA INDEX USING 2 GAP SIZE ANALYSIS-METHODS. Ieee Transactions on Geoscience and Remote Sensing, 33(3): 777-787.

Combal, B. et al., 2003. Retrieval of canopy biophysical variables from bidirectional reflectance - Using prior information to solve the ill-posed inverse problem. Remote Sensing of Environment, 84(1): 1-15.

Disney, M.I., Saich, P. and Lewis, P., 2003. Modelling the radiometric response of a dynamic, 3D structural model of Scots Pine in the optical and microwave domains. Igarss 2003: Ieee International Geoscience and Remote Sensing Symposium, Vols I - Vii, Proceedings: 3537-3539.

Espana, M., Baret, F., Aries, F., Andrieu, B. and Chelle, M., 1999. Radiative transfer sensitivity to the accuracy of canopy structure description. The case of a maize canopy. Agronomie, 19(3-4): 241-254.

Evers, J.B. et al., 2007. An architectural model of spring wheat: Evaluation of the effects of population density and shading on model parameterization and performance. Ecological Modelling, 200(3-4): 308-320.

Fournier, C. et al., 2005. A functional-structural model of elongation of the grass leaf and its relationships with the phyllochron. New Phytologist, 166(3): 881-894.

Garrigues, S. et al., 2008. Intercomparison and sensitivity analysis of Leaf Area Index retrievals from LAI-2000, AccuPAR, and digital hemispherical photography over croplands. Agricultural and Forest Meteorology, 148(8-9): 1193-1209.

Jonckheere, I. et al., 2004. Review of methods for in situ leaf area index determination - Part I. Theories, sensors and hemispherical photography. Agricultural and Forest Meteorology, 121(1-2): 19-35.

Knyazikhin, Y., Martonchik, J.V., Myneni, R.B., Diner, D.J. and Running, S.W., 1998. Synergistic algorithm for estimating vegetation canopy leaf area index and fraction of absorbed photosynthetically active radiation from MODIS and MISR data. Journal of Geophysical Research-Atmospheres, 103(D24): 32257-32275.

Lewis, P., 2007. 3D canopy modelling as a tool in remote-sensing research. Functional-Structural Plant Modelling in Crop Production, 22: 219-229.

Lopez-Lozano, R., Baret, F., de Cortazar-Atauri, I.G., Bertrand, N. and Casterad, M.A., 2009. Optimal geometric configuration and algorithms for LAI indirect estimates under row canopies: The case of vineyards. Agricultural and Forest Meteorology, 149(8): 1307-1316.

Louarn, G., Lebon, E. and Lecoeur, J., 2005. "Top-vine", a topiary approach based architectural model to simulate vine canopy structure. XIV International GESCO Viticulture Congress, Geisenheim, Germany, 23-27 August, 2005: 464-470.

Moran, M.S., Humes, K.S. and Pinter, P.J., 1997. The scaling characteristics of remotely-sensed variables for sparsely-vegetated heterogeneous landscapes. Journal of Hydrology, 190(3-4): 337-362.

Pradal, C., Dufour-Kowalski, S., Boudon, F., Fournier, C. and Godin, C., 2008. OpenAlea: a visual programming and component-based software platform for plant modelling. Functional Plant Biology, 35(9-10): 751-760.

Prusinkiewicz, P., 1999. A look at the visual modeling of plants using L-systems. Agronomie, 19(3-4): 211-224.

Weiss, M., Baret, F., Smith, G.J., Jonckheere, I. and Coppin, P., 2004. Review of methods for in situ leaf area index (LAI) determination Part II. Estimation of LAI, errors and sampling. Agricultural and Forest Meteorology, 121(1-2): 37-53.